Contents lists available at ScienceDirect

Inorganica Chimica Acta

Research paper

Ab initio study of structural and electronic properties of $Si_nC_{5-n}H_8$ (n = 0–5) series: Probing the 2D to 3D structural transition

İskender Muz [a,*], Mustafa Kurban [b]

[a] Faculty of Education, Department of Mathematics and Science Education, Nevsehir Haci Bektas Veli University, 50300 Nevsehir, Turkey
[b] Department of Electronics and Automation, Ahi Evran University, 40100 Kirsehir, Turkey

A B S T R A C T

In this study, we studied the structural and electronic properties in the $Si_nC_{5-n}H_8$ (n = 0–5) series using ab initio calculations. We performed global minimum and low-lying isomers search for the C_5H_8, SiC_4H_8, $Si_2C_3H_8$, $Si_3C_2H_8$, Si_4CH_8 and Si_5H_8 stoichiometries at the B3LYP/3-21G level of theory. The lowest isomers were recalculated at the CCSD(T)/CBS//B3LYP/6-311++G** level of theory. It was shown that $Si_2C_3H_8$ structure is more stable than the other structures with high ionization potential and HOMO-LUMO energy gap. We also showed the 2D-3D that transition, which occurs only at n = 3, is due to stronger C–C σ bonds compared to weaker C–Si and Si–Si σ bonds. The results were found in good agreement with available experimental findings.

© 2018 Elsevier B.V. All rights reserved.

1. Introduction

Systems containing hydrocarbons having strong covalent bonds are interesting because of their central role in organic chemistry. The simplest form of hydrocarbons are composed of carbon and hydrogen atoms bonded to a chain of carbon atoms [1]. Many hydrocarbons are actually combinations of chains and rings, or multiple rings linked together. An additional feature that adds diversity to hydrocarbon structures is the possibility of ring formation. For example, the cyclopentene structure of C_5H_8 has the lowest-energy among the many isomers of hydrocarbons [2–4]. In this regard, the ring arrangement of π-electrons in saturated conjugated compounds may cause a significant effect on the stability of the system [5–22].

Hydrogenated Si–C clusters would be very important for the understanding and modeling of the hydrogenated silicon-carbon alloys [23]. According to this viewpoint, the incorporation of Si atom into a hydrocarbon could induce a significant change in structural and electronic properties of the system. In the literature, a few types of silicon-containing CH compounds were studied. For example, the electronic structure of $Si_{1-x}C_xH$ was calculated and found the behavior of the alloys changes significantly at around x = 0.6 [24]. In the study, the results show that the bandgap decreases almost linearly with decreasing x. In addition, SiCH alloy based on the composition of Si atom is found to be a suitable mate-

rial for optoelectronic applications [25]. A recent study shows that hydrogenated Si–C honeycomb structure forms five stable isomers, and the chair conformer which remains stable even at room temperature is most stable [26]. Silicon and carbon substitution also gives rise to 2D-3D transition in series of SiC_5H_6 where benzene-like structures become considerably more stable than the other structures [27].

All the mentioned above examples indicate the role of silicon and carbon substitution in Si–C–H system and invite further investigation about the stability, electronic and structure properties of the system to obtain desirable properties. To our knowledge, the ring structure of hexasilabenzene which is similar to benzene has been recently studied in detail [27–30]. Moreover, a structural transition of hydrogenated and pure carbon clusters upon substitution of carbon by other elements have already examined [31,32]. However, the planar aromatic structures like benzene or its derivatives have not been synthesized in the compounds based on silicon. In this regard, a transition from two-dimensional (2D) to three-dimensional (3D) structures is searched in the $Si_nC_{5-n}H_8$ (n = 0–5) series upon sequential substitution of the C atoms by Si atoms in this study. In addition, the structural stability, chemical bonding, the adiabatic ionization potential (AIP), vertical ionization potential (VIP), HOMO-LUMO energy gap (E_g), adaptive natural density partitioning (AdNDP) and radial distribution function (RDF) of binary interactions of $Si_nC_{5-n}H_8$ (n = 0–5) series are investigated using density functional theory (DFT) based on optimized structure with the lowest energy among the studied isomers.

2. Computational details

The geometries of low-lying isomers of $Si_nC_{5-n}H_8$ (n = 0–5) series was performed using DFT with Becke's three-parameter exchange and Lee-Yang-Parr nonlocal correlation functional (B3LYP) [33]. For the geometry optimizations, about thirty isomers [34] of C_5H_8 stoichiometry are first carried out. To generate the structural isomers of other stoichiometries, the following procedures are used. The initial geometries are typically constructed by replacing one C atom by one Si atom in C_5H_8 stoichiometry. The obtained new isomers and their permutational isomers are optimized. This procedure continues until each carbon atom takes up the silicon atom, and then the entire series are optimized.

All possible structural patterns of considered series with singlet and triplet states are optimized at the B3LYP/3-21G level without any symmetry constraints. Then, the low-lying isomers for each series are reoptimized at the B3LYP/6-311++G** level. The frequency analysis is also performed at the same level to ensure the stability of all isomers. In order to get more accurate energies, the single-point calculations are performed using coupled cluster with single, double and perturbative triple excitations (CCSD(T)) functional in the CBS and aug-cc-pVXZ (X = D,T,Q) basis sets. All ab initio calculations were performed using the Gaussian 09 program package [35]. AdNDP calculation [36,37] has been used to explore electronic structure of closed-shell systems. Molecular structure and orbital visualizations are also performed with the GaussView 5.0.9 [38] and Molekel 5.4.0.8 [39] programs.

3. Results and discussion

In the present study, all the possible isomers of $Si_nC_{5-n}H_8$ (n = 0–5) series were examined by ab initio calculations. The cyclopentene, 1,3-pentadiene, 1,4-pentadiene, 1-methylcyclobutene, methylenecyclobutane, ethylidenecyclopropane, housane and bicyclopentane structures were found to be the lowest energy isomers of each series. Therefore, we have also separately considered the permutational isomers of each structure. All isomers were ordered according to their energies at the CCSD(T)/CBS//B3LYP/6-311++G** level of theory (see Fig. 1). Additionally, the relative energies (see Figs. S1–S6) and the total energies at B3LYP and CCSD(T) functionals (as Table S1), and the cartesian coordinates optimized at B3LYP/6-311++G** level of theory (see Table S2) for selected isomers are reported in Supporting Information. Note that all the optimized geometry of $Si_nC_{5-n}H_8$ (n = 0–5) series are found to be real minima because there are no imaginary frequencies.

C_5H_8 isomers. Despite the fact that four isomers for C_5H_8 stoichiometry: the cyclopentene, 1,3-pentadiene, 1,4-pentadiene, housane and bicyclopentane structures have been isolated and well-known [3,4,14,15]. The cyclopentene structure is found as the most stable among these isomers. In this study, the most stable isomer for C_5H_8 stoichiometry is found to be a cyclopentene (I.1) structure (C_s and 1-A configuration) being 1,3-pentadiene (I.2) structure (9.45 kcal/mol above the global minimum). The energies of the 1,4-pentadiene (I.3) and housane (I.7) structures are found to be as 16.15 and 29.23 kcal/mol, respectively, which are higher than that of the first isomer. The energy of the bicyclopentane (I.8) structure with D_{3h} point group symmetry is also found to be 39.07 kcal/mol which is higher than the global minimum (see Fig. 1).

SiC_4H_8 isomers. The cyclopentene-like (II.1) structure is very similar to the global minimum structure of C_5H_8 and only difference is that one C is substituted by the Si atom. Moreover, the energies of 1,3-pentadiene-like (II.4) and 1,4-pentadiene-like (II.5) structures are found to be 18.10 kcal/mol and 18.41 kcal/mol higher than the global minimum structure, respectively

(see Fig. 1). The energy of the bicyclopentane (II.6) structure (C_{3v} and 1-A1 configuration) is still significantly higher than cyclopentene-like structure (24.85 kcal/mol), but is now lower than that of housane-like (II.8) structure.

$Si_2C_3H_8$ isomers. In this size, the permutational isomers of each structure were examined in detail. Accordingly, the most stable isomer is still cyclopentene-like (or 1,3-disilacyclopentene) structure which is very similar to the global minimum structure of SiC_4H_8. The second isomer, bicyclopentane (III.2) structure, has D_{3h} point group symmetry, and it is now a close-lying (8.52 kcal/mol) the first isomer. Additionally, the energy of the 1,3-pentadiene-like (III.6) and 1,4-pentadiene-like (III.7) structures are now much higher than cyclopentene-like structure.

$Si_3C_2H_8$ isomers. Here we specially investigated the permutational isomers of cyclopentene-like and bicyclopentane structures. For the $Si_3C_2H_8$ stoichiometry, we found that bicyclopentane (IV.1) structure is now the global minimum with C_{2v} point group symmetry. The energy of the cyclopentene-like (IV.1) or 1,2,3-trisilacyclopentene structure is found to be 0.52, 2.79 and 2.98 kcal/mol at CCSD(T)/CBS//B3LYP/6-311++G**, CCSD(T)/aug-cc-pVQZ//B3LYP/6-311++G** and CCSD(T)/aug-cc-pVTZ//B3LYP/6-311++G** levels, respectively, which are higher energy than the global minimum structure. According to our calculations, the 2D-3D transition occurs at n = 3, where bicyclopentane structure becomes a little more stable than the nearest planar two-dimensional structure. On the other hand, the cyclopentene-like structure is the global minimum (at B3LYP/6-311++G** and CCSD(T)/aug-cc-pVDZ//B3LYP/6-311++G** levels (Supporting Information, Fig. S4); however, the single-point calculations indicate that planar cyclopentene-like (IV.2) structure is the second lowest isomer at CCSD(T)/CBS//B3LYP/6-311++G**, CCSD(T)/cc-pVQZ//B3LYP/6-311++G** and CCSD(T)/cc-pVTZ//B3LYP/6-311++G** levels, which are becoming more accurate and reliable (see Fig. 1). Note that the relative energies obtained by the CCSD(T)/cc-pVTZ//B3LYP/6-311++G**, CCSD(T)/aug-cc-pVQZ//B3LYP/6-311++G** and CCSD(T)/CBS//B3LYP/6-311++G** levels are compatible with each series. In addition, the energies of the housane-like (IV.5), 1,3-pentadiene-like (IV.7) and 1,4-pentadiene (I.8) structures are found to be 24.12, 43.16 and 46.21 kcal/mol, respectively, which are higher than the global minimum (see Fig. 1).

Si_4CH_8 isomers. The most stable isomer for Si_4CH_8 has a bicyclopentane (V.1) structure (C_{2v} and 1-A1 configuration) being cyclopentene-like (V.2) structure (7.83 kcal/mol above the global minimum). The energy of the housane-like (V.3) structure is now 10.64 kcal/mol which is higher than global minimum structure. Moreover, 1,3-pentadiene-like (V.7) and 1,4-pentadiene (V.8) structures are found to be 47.45 and 49.36 kcal/mol, respectively. These energy values are higher than the most stable isomer (Fig. 1).

Si_5H_8 isomers. The bicyclopentane (VI.1) structure (D_{3h} and 1-A1′ configuration) is significantly more stable than the other isomers. The energy of the housane-like (VI.2) structure is found to be 14.87 kcal/mol which is higher than the first isomer. The global minimum of Si_5H_8 stoichiometry has been reported by Li et al. [40]. The most stable isomer presented in our work is in excellent agreement with those found in literature [40]. Additionally, the energies of the cyclopentene-like (VI.3), 1,3-pentadiene-like (VI.7) and 1,4-pentadiene-like (VI.8) structures are 17.17, 58.23 and 62.52 kcal/mol, respectively. These values are higher than the global minimum (see Fig. 1). From the results mentioned above, we can conclude that the most stable isomers of the carbon-rich series are cyclopentene-like structure with 2D, whereas the most stable isomers of silicon-rich series are bicyclopentane structure with 3D.

Bond lengths. All bond lengths for the most stable isomers are shown in Fig. 2. In $Si_nC_{5-n}H_8$ series, C = C double bond lengths for

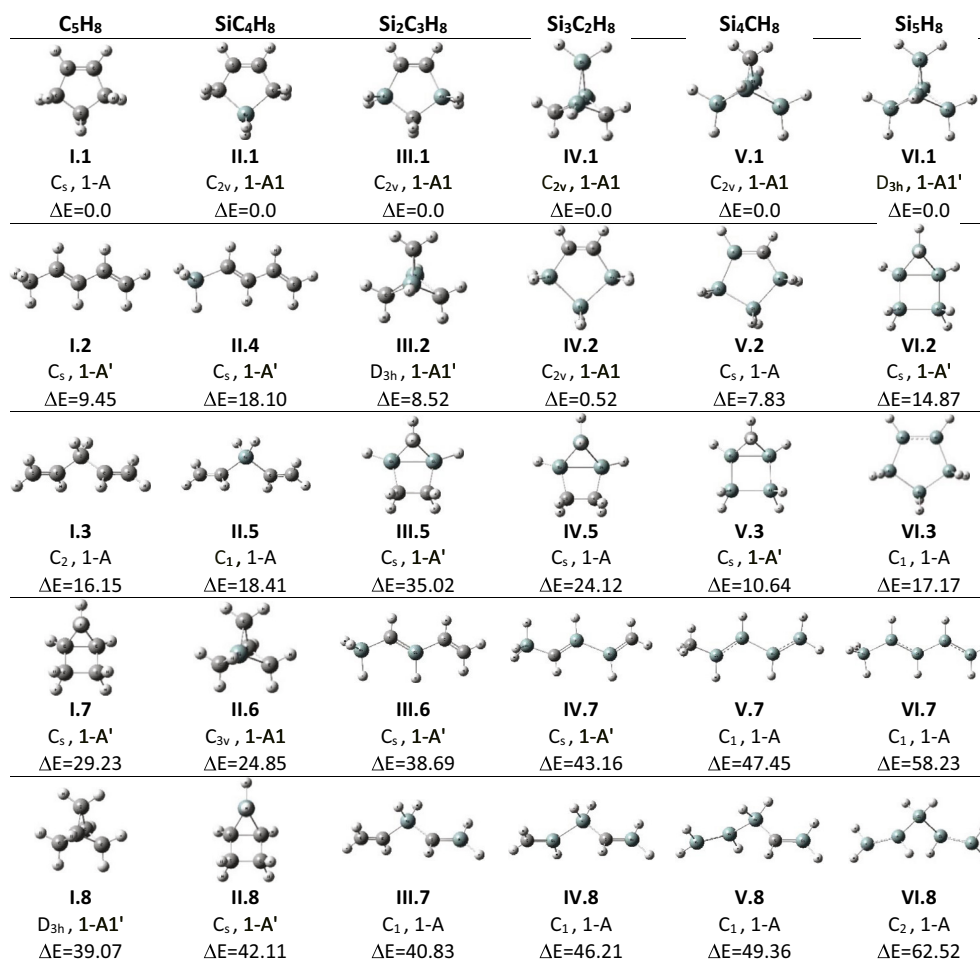| C₅H₈	SiC₄H₈	Si₂C₃H₈	Si₃C₂H₈	Si₄CH₈	Si₅H₈
I.1 C_s, 1-A $\Delta E=0.0$	**II.1** C_{2v}, 1-A1 $\Delta E=0.0$	**III.1** C_{2v}, 1-A1 $\Delta E=0.0$	**IV.1** C_{2v}, 1-A1 $\Delta E=0.0$	**V.1** C_{2v}, 1-A1 $\Delta E=0.0$	**VI.1** D_{3h}, 1-A1' $\Delta E=0.0$
I.2 C_s, 1-A' $\Delta E=9.45$	**II.4** C_s, 1-A' $\Delta E=18.10$	**III.2** D_{3h}, 1-A1' $\Delta E=8.52$	**IV.2** C_{2v}, 1-A1 $\Delta E=0.52$	**V.2** C_s, 1-A $\Delta E=7.83$	**VI.2** C_s, 1-A' $\Delta E=14.87$
I.3 C_2, 1-A $\Delta E=16.15$	**II.5** C_1, 1-A $\Delta E=18.41$	**III.5** C_s, 1-A' $\Delta E=35.02$	**IV.5** C_s, 1-A $\Delta E=24.12$	**V.3** C_s, 1-A' $\Delta E=10.64$	**VI.3** C_1, 1-A $\Delta E=17.17$
I.7 C_s, 1-A' $\Delta E=29.23$	**II.6** C_{3v}, 1-A1 $\Delta E=24.85$	**III.6** C_s, 1-A' $\Delta E=38.69$	**IV.7** C_s, 1-A' $\Delta E=43.16$	**V.7** C_1, 1-A $\Delta E=47.45$	**VI.7** C_1, 1-A $\Delta E=58.23$
I.8 D_{3h}, 1-A1' $\Delta E=39.07$	**II.8** C_s, 1-A' $\Delta E=42.11$	**III.7** C_1, 1-A $\Delta E=40.83$	**IV.8** C_1, 1-A $\Delta E=46.21$	**V.8** C_1, 1-A $\Delta E=49.36$	**VI.8** C_2, 1-A $\Delta E=62.52$

Fig. 1. The relative energies (kcal/mol) according to energies at the CCSD(T)/CBS level of theory as well as the point group symmetries and electronic states of $Si_nC_{5-n}H_8$ (n = 0–5) series. Each energy includes ZPE corrections.

the cyclopentane-like structures increase marginally (from 1.333 to 1.347 Å) in range of n = 0–2, whereas, C–Si bond lengths decrease from 1.907 (at n = 1) to 1.885–1.898 Å (at n = 2). After transition to bicyclopentane like structures, there is no systematic change in Si–Si bond lengths. Firstly, Si–Si bond lengths increase from 1.922 (at n = 3) to 2.407 Å (at n = 4) in range of n = 3–4 and then decrease from 2.407 (at n = 4) to 2.363 Å (at n = 5) in range of n = 4–5. In addition, there is no considerable change in the C–H and Si–H bond lengths with respect to the substitution of carbon atoms by silicon atoms. Fig. 3 shows that our study and experimental electron diffraction data [41] are in good agreement for the bond distances and angles of cyclopentene structure.

Charge transfers. The charge transfer is highly important for the reactivity of the atoms or molecules in the clusters. Thus, the intermolecular charge transfers are investigated at B3LYP/6-311+ +G** level of calculation using the electrostatic potential (ESP) and natural population (NPA) analyses [42]. The results of our analysis for $Si_nC_{5-n}H_8$ (n = 0–5) series are presented in Fig. 4(a-b). All the charges for the C₅H₈ are nearly on the H atoms, and the charge transfer is small. Moreover, the charges are transferred from hydrogen to carbon. The charge transfers increase in range of n = 1–2 with a large peak for n = 2, but starting to decrease in range of n = 3–4. After at n = 5, all of the charges are on the silicon atoms, and the charges are transferred from silicon to hydrogen. Because of the fact that a complete transfer of electrons from the more electropositive atom to the more electronegative atom, the general trend of the charges for carbon-rich series and silicon-rich series

are transferred from hydrogen atoms to carbon atoms, whereas, those for silicon-rich series are transferred from silicon atoms to hydrogen atoms, respectively (see Fig. 4a-b). ESP charge distributions are also found to be compatible with NPA charge distributions.

Structural stability and electronic properties. In order to probe the structural stabilities of $Si_nC_{5-n}H_8$ series, we used the binding energy per atom (E_b) and second-order energy difference (Δ^2E). The E_b and Δ^2E can be calculated from the first and second formulas, respectively.

$$E_b = [(n \times E_{Si} + (5-n) \times E_C + 8 \times E_H) - (E_{Si_nC_{5-n}H_8})]/13 \quad (1)$$

where index n (the number of Si atoms) is from 0 to 5, E_{Si} is the energy of atomic silicon, E_C is the energy of atomic carbon, E_H is the energy of atomic hydrogen and $E_{Si_nC_{5-n}H_8}$ is the cluster energy, and

$$\Delta^2E_n = E_{n+1} + E_{n-1} - 2(E_n) \quad (2)$$

where n (the number of Si atoms) is from 1 to 4, and E_n, E_{n+1} and E_{n-1} correspond to the total energy of related series. As seen in Fig. 5(a), the E_b and Δ^2E values are plotted as a function of n. From Fig. 5(a), the substitution of carbon atoms by silicon atoms in considered series smoothly decreases the E_b from 0.18 to 0.12 eV. Moreover, Δ^2E exhibits the odd-even oscillating behavior and a sharp peak occurs at Si₂C₃H₈, indicating the highest stability of this group. In order to investigate the electronic properties of considered
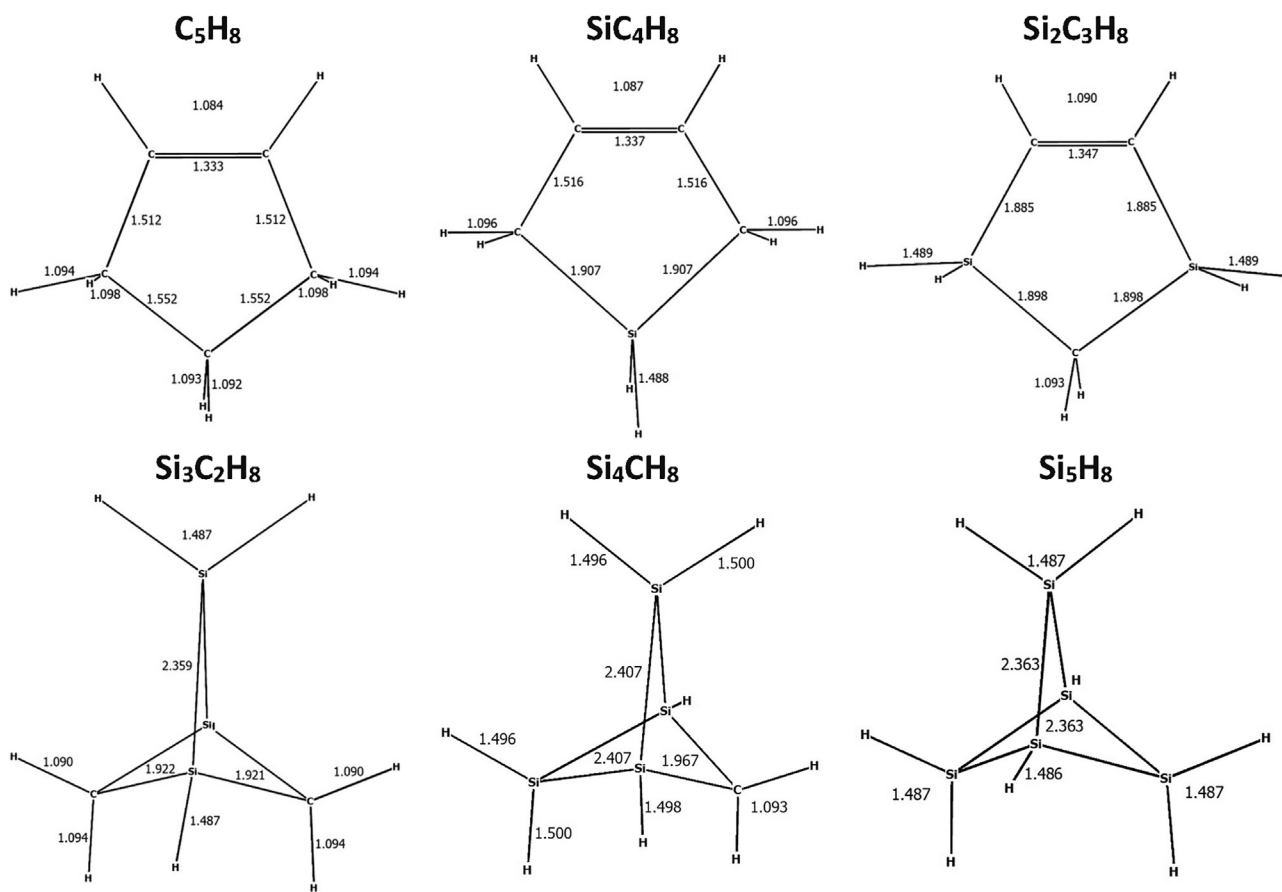
Fig. 2. Bond lenghts for the most stable isomers of $Si_nC_{5-n}H_8$ (n = 0–5) series.
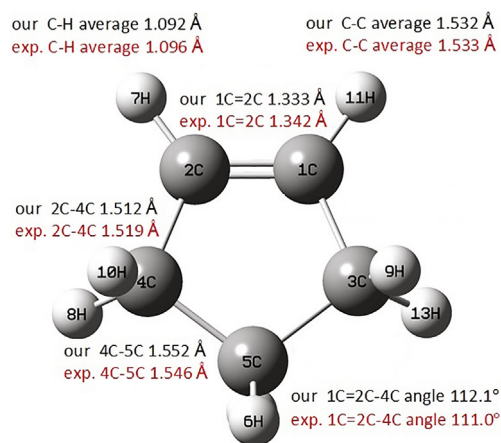

Fig. 3. Bond distances and angles obtained in our study and experimental data from electron diffaction [41] for the cyclopentene structure.

series, we also calculated the AIP, VIP and E_g. The AIP and VIP can be calculated separately from the third formula.

$$AIP/VIP = E(cation) - E(neutral) \qquad (3)$$

where AIP is the energy difference between the ground state of the optimized cation and the ground state of the optimized neutral, and VIP is the energy difference between the ground state of the cation and the ground state of the neutral which optimized by the geometry of the neutral. AIP, VIP and E_g values are plotted as a function of

n, in Fig. 5(b). Moreover, AIP, VIP and E_g values together with E_b are listed in Table 1. It can be seen that AIP, VIP and E_g values generally increase in range of n = 0–2 with a peak for n = 2, but starting to decrease in range of n = 3–4 with a large dip for n = 4, and then again increase at n = 5. Note that as a result of orbital relaxation on ionization, the VIP values are higher than the AIP values because of energy compensation. Moreover, the AIP and VIP values exhibit the similar trend with E_g values. According to these results, the $Si_2C_3H_8$ stoichiometry is more stable with higher values of AIP, VIP and E_g, whereas the Si_4CH_8 stoichiometry is the least stable compared to the other series. C–C bond is perfectly covalent whereas Si–C bond is partially ionic. As the number of partially ionic bond increases, the HOMO-LUMO gap increases. From these results, one can conclude that not only relatively large ionization potential as a criterion of stability but also relatively large HOMO-LUMO energy separation against electronic excitations have an effect on the stability. According to our calculation, the calculated the highest ionization potential (AIP = 9.15 eV and VIP = 9.69 eV) for $Si_2C_3H_8$ series reveals it as the most stable structure. Therefore, it can be explained by reasons such as the hybridization of orbitals and increase in ionicity of the bonds. Although B3LYP underestimates HOMO-LUMO gaps [43–46], but range-separated functionals are a way to correct for this deficiency, the calculated relative energies obtained from B3LYP is found to be compatible with that of CCSD (T) in this study. In addition, the present calculated VIP of C_5H_8 (9.00 eV) is also good agreement with experimental value of 9.01 ± 0.01 eV from literature [3,47–49]. To date there have been no any experimental data related with the other series, thus VIPs results for the other series obtained from this study could be useful for the future studies.
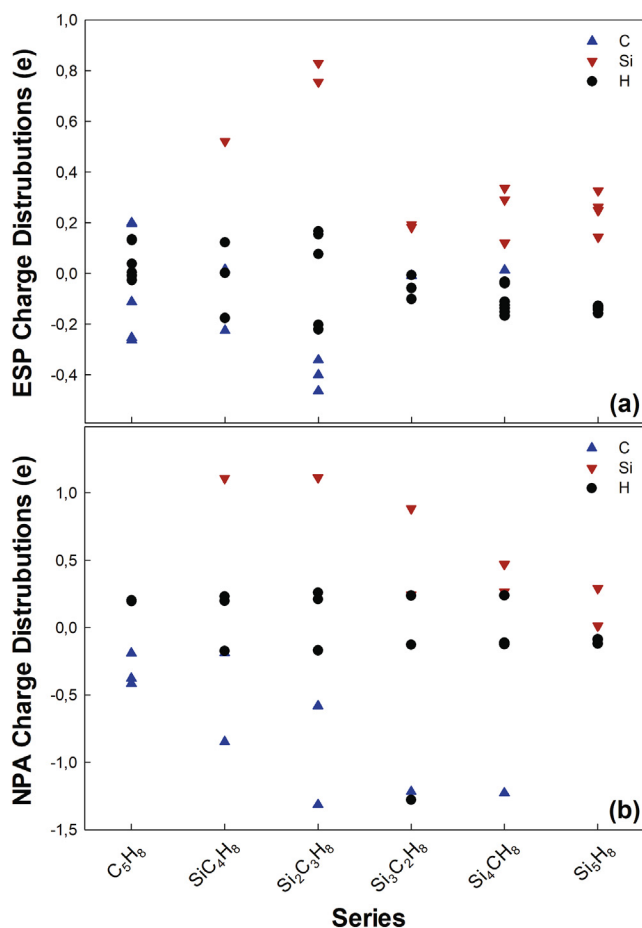
Fig. 4. The charge distributions for $Si_nC_{5-n}H_8$ series (a) ESP (b) NPA.

Fig. 5. For $Si_nC_{5-n}H_8$ (n = 0–5) series (a) The binding energy per atom (E_b/atom) and second-order energy difference (Δ^2E) (b) the adiabatic/vertical ionization potentials (AIP/VIP) and HOMO-LUMO energy gap (E_g).

Table 1
The binding energy per atom (E_b), adiabatic ionization potential (AIP), vertical ionization potential (VIP) and HOMO-LUMO energy gap (E_g). All values in eV.

Size	E_b	AIP	VIP	E_g
C_5H_8	0.18	8.64	9.00	6.44
SiC_4H_8	0.17	8.60	9.16	6.62
$Si_2C_3H_8$	0.16	9.15	9.69	6.71
$Si_3C_2H_8$	0.15	8.20	8.68	6.18
Si_4CH_8	0.14	8.13	8.45	5.82
Si_5H_8	0.12	8.35	8.71	6.01

AdNDP analyses. The AdNDP analysis can be used to interpret the molecular orbitals because of a very efficient visual approach and an extension of the natural bond orbital (NBO) analysis. It searches the core electron pairs and n-center two-electron (nc-2e) bonds as well as the occupation numbers (ONs) in the molecular orbitals. Moreover, it is not sensitive for the method and basis set. We performed the AdNDP analysis for the most stable isomers using B3LYP functional with LANL2DZ basis set. The results of our analysis are pictured in Fig. 6.

For the C_5H_8 global minimum structure I.1, we found five 2c-2e C–C σ bonds with ON = 1.98–1.99|e|, eight 2c-2e C–H σ bonds (ON = 1.97–1.98|e|) and one 2c-2e C–C π bond (ON = 1.95|e|). The SiC_4H_8 global minimum structure II.1 has three 2c-2e C–C σ bonds with ON = 1.98–1.99|e|, six 2c-2e C–H σ bonds (ON = 1.97–1.98|e|), two 2c-2e C–Si σ bonds (ON = 1.97|e|), two 2c-2e Si–H σ bonds (ON = 1.99|e|) and one 2c-2e C–C π bond (ON = 1.96|e|). For the $Si_2C_3H_8$ global minimum structure III.1, we found one 2c-2e C–C σ bonds with ON = 1.99|e|, four 2c-2e C–H σ bonds (ON = 1.98–1.99|e|), four 2c-2e C–Si σ bonds (ON = 1.97–1.98|e|), four 2c-2e Si–H σ bonds (ON = 1.99|e|) and one 2c-2e C–C π bond (ON = 1.96|e|). The $Si_3C_2H_8$ global minimum structure IV.1 has four 2c-2e C–H σ bonds with ON = 1.99|e|, four 2c-2e C–Si σ bonds (ON = 1.97|e|), four 2c-2e Si–H σ bonds (ON = 1.99|e|) and two 2c-2e Si–Si σ bonds (ON = 1.94|e|). For the Si_4CH_8 global minimum structure V.1, we found two 2c-2e C–H σ bonds with ON = 1.99|e|, two 2c-2e C–Si σ bonds (ON = 1.97|e|), six 2c-2e Si–H σ bonds (ON = 1.99|e|) and four 2c-2e Si–Si σ bonds (ON = 1.94|e|). The Si_5H_8 global minimum structure VI.1 has eight 2c-2e Si–H σ bonds with ON = 1.99|e| and six 2c-2e Si–Si σ bonds with ON = 1.60|e|. AdNDP
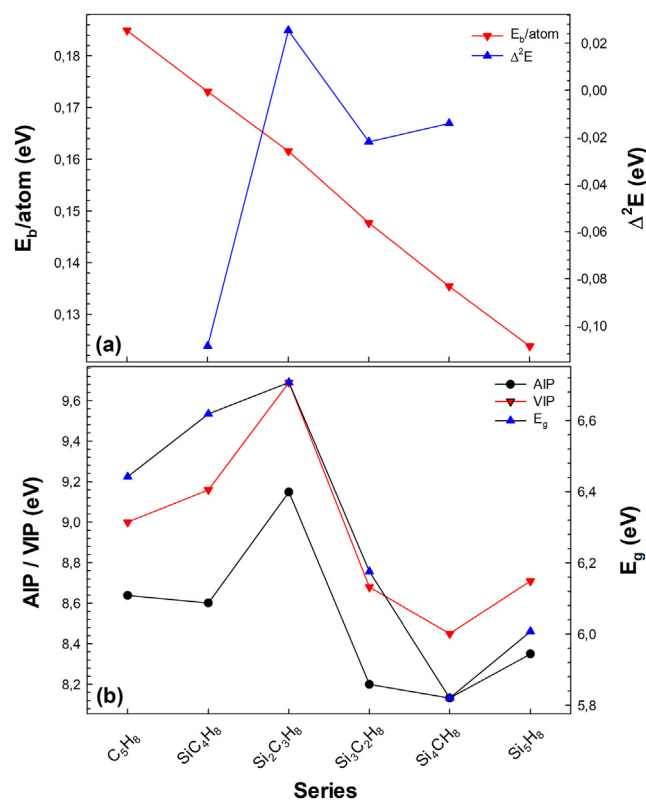
calculations show that the most stable isomers of the carbon-rich series prefer both 2c-2e σ and 2c-2e π bonds, however; the most stable isomers of the silicon-rich prefer only 2c-2e σ bonds. In short, AdNDP analysis of the most stable isomers is in agreement with the intuitive valence bond structures of these molecules, this analysis yields the expected 2c-2e bonds with populations of close to two electrons and the expected symmetry of orbital interactions as either σ- or π-bonds. Moreover, ONs values for the most stable isomers are very close to the ideal values. In this study, we also are confident the results obtained on the chemical bonding patterns.

Radial distribution function analyses. The radial distribution functions (RDF) give the probability of finding a particle in the distance from another particle. In this study, the purpose of the RDF is to determine the effect of silicon and carbon concentrations on the binary interactions in the $Si_nC_{5-n}H_8$ (n = 0–5) series. In this regard, we performed the RDF analysis for carbon-carbon (C–C), carbon-hydrogen (C–H), hydrogen-hydrogen (H–H), carbon-silicon (C–Si) and silicon-hydrogen (Si–H) interactions of $Si_nC_{5-n}H_8$ (n = 0–5) series (see Fig. 7(a-f)). The RDFs are calculated for each binary atomic pairs of the most stable isomers of $Si_nC_{5-n}H_8$ (n = 0–5) series. The
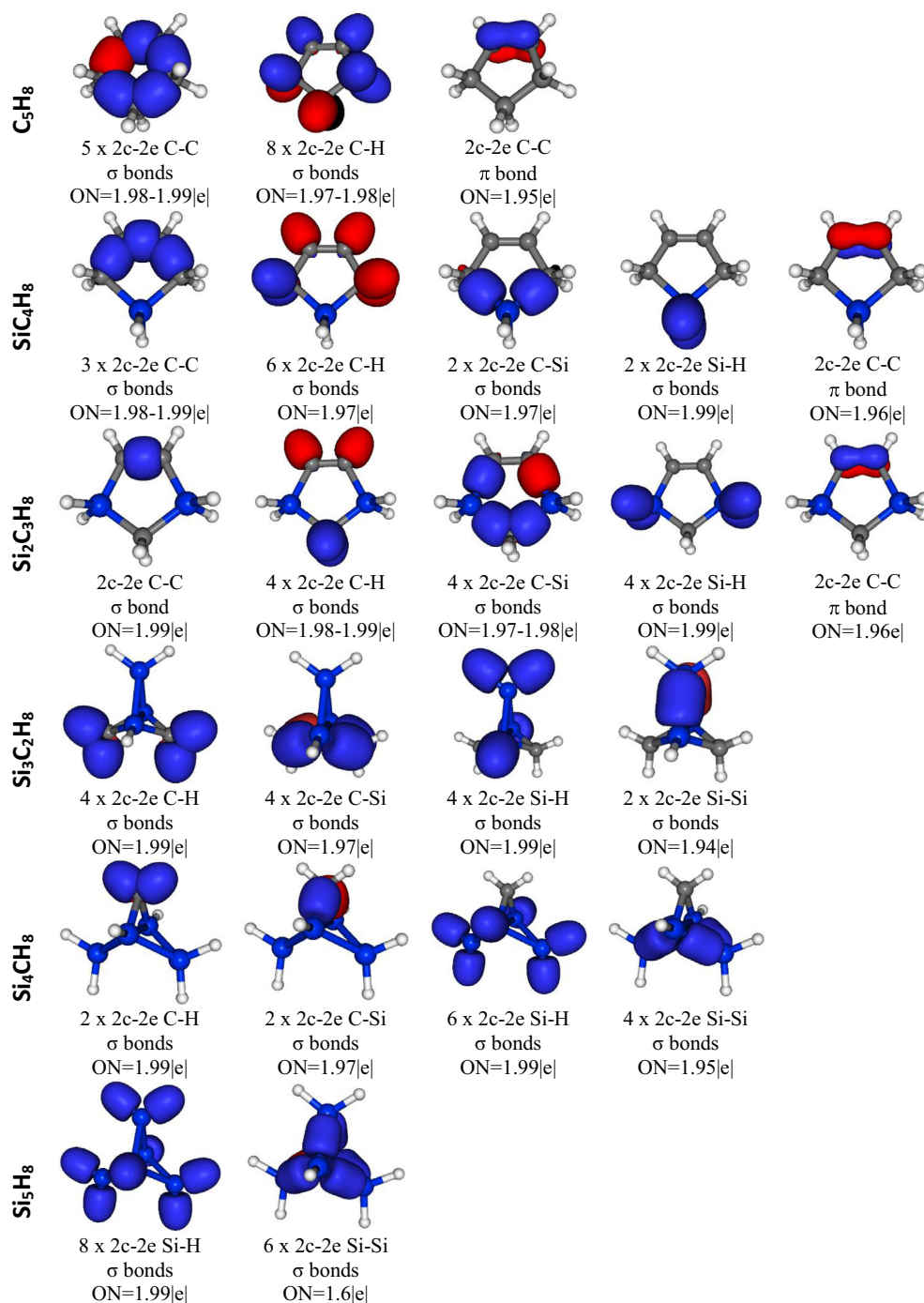
Fig. 6. Chemical bonding patterns of the most stable isomers recovered by AdNDP analysis.

RDF of the same binary interactions in the different compositions shows different behavior. For example, the RDF of C–H interactions has a narrower and higher distribution for SiC_4H_8; however, the interactions are smaller than that of C–C and C–Si for $Si_2C_3H_8$. This behavior is found to be compatible with the decrease of the binding energy per atom which decreases with substitution of the carbon atoms. In addition, there is a slight difference between C–C and C–Si atoms for SiC_4H_8, $Si_2C_3H_8$ and $Si_3C_2H_8$. For C atoms, C–C is greater than C–Si interactions; for H, Si–H is shorter than C–H; for Si, Si–H is slightly shorter than C–Si. For all of the combinations, C–H has stronger interactions than the other ones.

4. Conclusions

We presented a systematic study of the $Si_nC_{5-n}H_8$ series using B3LYP-DFT and CCSD(T) methods. We performed global minimum and low-lying isomers search for the C_5H_8, SiC_4H_8, $Si_2C_3H_8$, $Si_3C_2H_8$, Si_4CH_8 and Si_5H_8 stoichiometries at the B3LYP/3-21G level of theory. The lowest isomers were recalculated at the CCSD(T)/CBS//B3LYP/6-311++G** level of theory. The 2D-3D that transition, which occurs only at n = 3, where bicyclopentane structure becomes a little more stable than cyclopentene-like structure, is due to stronger C–C σ bonds compared to weaker
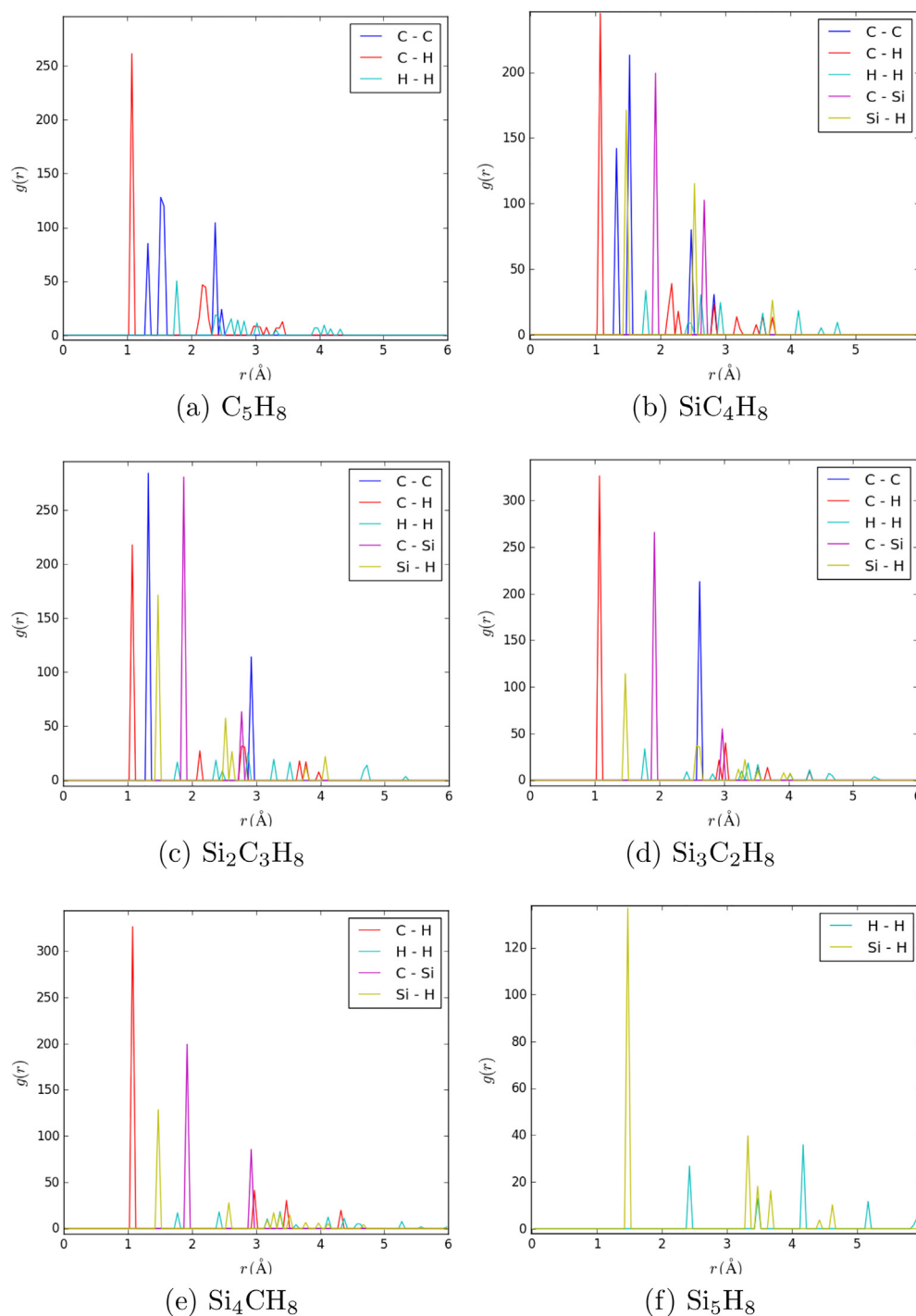
Fig. 7. Radial distribution function (RDF) between carbon–carbon (C–C), carbon–hydrogen (C–H), hydrogen–hydrogen (H–H), carbon–silicon (C–Si) and silicon–hydrogen (Si–H) interactions. (a) C_5H_8, (b) SiC_4H_8, (c) $Si_2C_3H_8$, (d) $Si_3C_2H_8$, (e) Si_4CH_8, (f) Si_5H_8.

C–Si and Si–Si σ bonds. The most stable isomers of the carbon-rich series (at n = 0–2) are cyclopentene-like structures with two-dimensional (2D), whereas the most stable isomers of silicon-rich series (at n = 3–5) are bicyclopentane structure with three-dimensional (3D). From the energetic point of view, the binding energy decreases with substitution of the carbon atoms by the silicon atoms. Moreover, the $Si_2C_3H_8$ stoichiometry is relatively more stable than the others with high IP and high HOMO-LUMO energy gap. From our results, the calculated relative energies calculated obtained from the B3LYP method are compatible with that of CCSD(T). In addition, C–H interactions have a narrower and higher distribution due to the weaker bond and the low atomic weight of the H atom. The results of our calculations for C_5H_8 are in excellent agreement with the experimental data. Therefore, our study could be useful for the future researches. Structural stability of cluster allows their presence in nature and afterwards to synthesize them in experiments. Therefore, we hope that current study will ultimately guide to designing and synthesizing a series of novel compound derivatives based on hydrogenated carbon-silicon for the future researches.

Appendix A. Supplementary data

Supplementary data associated with this article can be found, in the online version, at https://doi.org/10.1016/j.ica.2018.03.008.

References

[1] M. Menon, E. Richter, A. Mavrandonakis, G. Froudakis, A. Andriotis, Structure and stability of SiC nanotubes, Phys. Rev. B 69 (11) (2004), https://doi.org/10.1103/PhysRevB.69.115322. 115322.

[2] C. Szmytkowski, S. Stefanowska, M. Zawadzki, E. Ptasinska-Denga, P. Mozejko, Electron scattering from 2-methyl-1,3-butadiene, C5H8, molecules: Role of methylation, Phys. Rev. A 94 (4) (2016), https://doi.org/10.1103/PhysRevA.94.042706. 042706.

[3] N. Hansen, S. Klippenstein, J. Miller, J. Wang, T. Cool, M. Law, et al., Identification of C5Hx isomers in fuel-rich flames by photoionization mass spectrometry and electronic structure calculations, J. Phys. Chem. A 110 (13) (2006) 4376–4388, https://doi.org/10.1021/jp0569685.

[4] M. Leong, V. Mastryukov, J. Boggs, Structure and conformation of cyclopentene, cycloheptene and trans-cyclooctene, J. Mol. Struct. 445 (1–3) (1998) 149–160, https://doi.org/10.1016/S0022-2860(98)00421-9.

[5] M. Balci, M. McKee, P. Schleyer, Theoretical study of tetramethyl- and tetra-tert-butyl-substituted cyclobutadiene and tetrahedrane, J. Phys. Chem. A 104 (6) (2000) 1246–1255, https://doi.org/10.1021/jp9922054.

[6] K. Baldridge, O. Uzan, J. Martin, The silabenzenes: structure, properties, and aromaticity, Organometallics 19 (8) (2000) 1477–1487, https://doi.org/10.1021/om9903745.

[7] W. Freeman, T. Tilley, L. LiableSands, A. Rheingold, Synthesis and study of cyclic pi-systems containing silicon and germanium. The question of aromaticity in cyclopentadienyl analogues, J. Am. Chem. Soc. 118 (43) (1996) 10457–10468, https://doi.org/10.1021/ja962103g.

[8] E. Jemmis, P. Schleyer, Aromaticity in 3 dimensions .4. influence of orbital compatibility on the geometry and stability of capped annulene rings with 6 interstitial electrons, J. Am. Chem. Soc. 104 (18) (1982) 4781–4788, https://doi.org/10.1021/ja00382a008.

[9] J. Poater, R. Visser, M. Sola, F.M. Bickelhaupt, Polycyclic benzenoids: why kinked is more stable than straight, J. Organic Chem. 72 (4) (2007) 1134–1142, https://doi.org/10.1021/jo061637p.

[10] P. Schleyer, M. Manoharan, Z. Wang, B. Kiran, H. Jiao, R. Puchta, et al., Dissected nucleus-independent chemical shift analysis of pi-aromaticity and antiaromaticity, Organic Lett. 3 (16) (2001) 2465–2468, https://doi.org/10.1021/ol016217v.

[11] S.C.A.H. Pierrefixe, F.M. Bickelhaupt, Aromaticity: molecular-orbital picture of an intuitive concept, Chem.-A Eur. J. 13 (22) (2007) 6321–6328, https://doi.org/10.1002/chem.200700206.

[12] K. Fuchibe, H. Imaoka, J. Ichikawa, Synthesis of pinpoint-fluorinated polycyclic aromatic hydrocarbons: benzene ring extension cycle involving microwave-assisted SNAr reaction, Chem.-An Asian J. 12 (18) (2017) 2359–2363, https://doi.org/10.1002/asia.201700870.

[13] T. Fujita, I. Takahashi, M. Hayashi, J. Wang, K. Fuchibe, J. Ichikawa, Facile synthesis of polycyclic aromatic hydrocarbons: BrOnsted acid catalyzed dehydrative cycloaromatization of carbonyl compounds in 1,1,1,3,3,3-Hexafluoropropan-2-ol, Eur. J. Organic Chem. 2 (2017) 262–265, https://doi.org/10.1002/ejoc.201601406.

[14] O. Herbinet, A. Rodriguez, B. Husson, F. Battin-Leclerc, Z. Wang, Z. Cheng, et al., Study of the formation of the first aromatic rings in the pyrolysis of cyclopentene, J. Phys. Chem. A 120 (5) (2016) 668–682, https://doi.org/10.1021/acs.jpca.5b09203.

[15] S. Peter, M. Guenther, F. Richter, A comparative analysis of a-C: H films deposited from five hydrocarbons by thermal desorption spectroscopy, Vacuum 86 (6, SI) (2012) 667–671, https://doi.org/10.1016/j.vacuum.2011.07.037.

[16] V.V. Kislov, A.M. Mebel, J. Aguilera-Iparraguirre, W.H. Green, Reaction of phenyl radical with propylene as a possible source of indene and other polycyclic aromatic hydrocarbons: an Ab Initio/RRKM-ME study, J. Phys. Chem. A 116 (16) (2012) 4176–4191, https://doi.org/10.1021/jp212338g.

[17] H. Detert, D. Lenoir, H. Zipse, Thermal rearrangements of perchlorohexatrienes-structures and experimental and theoretical evaluation of pathways to isomerization and cyclization, Eur. J. Organic Chem. 8 (2009) 1181–1190, https://doi.org/10.1002/ejoc.200801076.

[18] V. Teberekidis, M. Sigalas, Structure and stability of halonium cations of cycloalkenes. A theoretical study, Tetrahedron 59 (26) (2003) 4749–4756, https://doi.org/10.1016/S0040-4020(03)00695-1.

[19] V. Teberekidis, M. Sigalas, Density functional study of potential energy surfaces and relative stabilities of halonium cations of ethylene and cyclopentenes, Tetrahedron 58 (31) (2002) 6171–6178, https://doi.org/10.1016/S0040-4020(02)00617-8.

[20] D. Birney, S. Ham, G. Unruh, Pericyclic and pseudopericyclic thermal cheletropic decarbonylations: when can a pericyclic reaction have a planar, pseudopericyclic transition state?, J Am. Chem. Soc. 119 (19) (1997) 4509–4517, https://doi.org/10.1021/ja963551r.

[21] I. Muz, M. Atis, Structural transformations in the carborane series: CnB6-nH6 (n=0–6) upon substitution of boron by carbon, Inorganica Chimica Acta 453 (2016) 626–632, https://doi.org/10.1016/j.ica.2016.09.035.

[22] T.R. Galeev, A.I. Boldyrev, Planarity takes over in the CxHxP6-x (x=0–6) series at x=4, Phys. Chem. Chem. Phys. 13 (46) (2011) 20549–20556, https://doi.org/10.1039/c1cp21959f.

[23] G. Ambrosone, U. Coscia, S. Ferrero, F. Giorgis, P. Mandracci, C. Pirri, Structural and optical properties of hydrogenated amorphous silicon-carbon alloys grown by plasma-enhanced chemical vapour deposition at various rf powers, Philos. Magazine B-Phys. Condensed Matter Statist. Mech. Electronic Optical Magnetic Properties 82 (1) (2002) 35–46, https://doi.org/10.1080/13642810110069279.

[24] J. Robertson, The electronic and atomic-structure of hydrogenated amorphous Si-C all, Philos. Magazine B-Phys. Condensed Matter Statist. Mech. Electronic Optical Magnetic Properties 66 (5) (1992) 615–638, https://doi.org/10.1080/13642819208207664.

[25] A. Skumanich, A. Frova, N. Amer, Urbach tail and gap stated in hydrogenated A-SiC and A-Sige alloys, Solid State Commun. 54 (7) (1985) 597–601, https://doi.org/10.1016/0038-1098(85)90086-9.

[26] S. Banerjee, C. Majumder, Conformers of hydrogenated SiC honeycomb structure: a first principles study, AIP Adv. 3 (8) (2013), https://doi.org/10.1063/1.4820389. 082136.

[27] A.S. Ivanov, A.I. Boldyrev, Si6-nCnH6 (n=0–6) series: when do silabenzenes become planar and global minima?, J Phys. Chem. A 116 (38) (2012) 9591–9598, https://doi.org/10.1021/jp307722q.

[28] A.D. Gupta, J.S. Arora, DFT evidence of unforeseen bending in linearly fused polycyclic rings of hexasilabenzenoids, Comput. Theor. Chem. 1099 (2017) 87–91, https://doi.org/10.1016/j.comptc.2016.11.010.

[29] K. Abersfelder, A.J.P. White, R.J.F. Berger, H.S. Rzepa, D. Scheschkewitz, A Stable Derivative of the Global Minimum on the Si6H6 Potential Energy Surface, Angewandte Chemie-International Edition 50 (34) (2011) 7936–7939, https://doi.org/10.1002/anie.201102623.

[30] K. Abersfelder, A tricyclic aromatic isomer of hexasilabenzene, Science 331 (6015) (2011) 284, https://doi.org/10.1126/science.1181771.

[31] T.R. Galeev, A.S. Ivanov, C. Romanescu, W.-L. Li, K.V. Bozhenko, L.-S. Wang, et al., Molecular wheel to monocyclic ring transition in boron-carbon mixed clusters C2B6- and C3B5-, Phys. Chem. Chem. Phys. 13 (19) (2011) 8805–8810, https://doi.org/10.1039/c1cp20359b.

[32] L.-M. Wang, B.B. Averkiev, J.A. Ramilowski, W. Huang, L.-S. Wang, A.I. Boldyrev, Planar to linear structural transition in small boron-carbon mixed clusters: CxB5-x- (x=1–5), J. Am. Chem. Soc. 132 (40) (2010) 14104–14112, https://doi.org/10.1021/ja103846q.

[33] A. Becke, Density-Functional Thermochemistry. III. The Role of Exact Exchange, J. Chem. Phys. 98 (1993) 5648–5652, https://doi.org/10.1063/1.464913.

[34] NIST Chemistry WebBook. URL http://webbook.nist.gov/cgi/cbook.cgi?Formula=c5h8&NoIon=on&Units=SI#.

[35] M.J. Frisch, G.W. Trucks, H.B. Schlegel, G.E. Scuseria, M.A. Robb, J.R. Cheeseman, et al., Gaussian09 Revision E.01, Gaussian Inc., Wallingford CT, 2009.

[36] D.Y. Zubarev, A.I. Boldyrev, Developing paradigms of chemical bonding: adaptive natural density partitioning, Phys. Chem. Chem. Phys. 10 (34) (2008) 5207–5217, https://doi.org/10.1039/b804083d.

[37] D.Y. Zubarev, A.I. Boldyrev, Revealing intuitively assessable chemical bonding patterns in organic aromatic molecules via adaptive natural density partitioning, J. Organic Chem. 73 (23) (2008) 9251–9258, https://doi.org/10.1021/jo801407e.

[38] R. Dennington, T.A. Keith, J.M. Millam, GaussView Version 5.0.9, Semichem Inc., Shawnee Mission KS, 2009.

[39] U. Varetto, Molekel 5.4.0.8, Swiss National Supercomputing Centre: Lugano (Switzerland).

[40] C.P. Li, X.J. Li, J.C. Yang, Silicon hydride clusters Si5H(n) (n=3–12) and their anions: Structures, thermochemistry, and electron affinities, J. Phys. Chem. A 110 (43) (2006) 12026–12034, https://doi.org/10.1021/jp064502w.

[41] M.I. Davis, T.W. Muecke, Molecular structure study of cyclopentene, J. Phys. Chem. 74 (5) (1970) 1104–1108, https://doi.org/10.1021/j100700a024.

[42] A. Reed, R. Weinstock, F. Weinhold, Natural-Population Analysis, J. Chem. Phys. 83 (2) (1985) 735–746, https://doi.org/10.1063/1.449486.

[43] M.E. Foster, B.M. Wong, Nonempirically Tuned Range-Separated DFT Accurately Predicts Both Fundamental and Excitation Gaps in DNA and RNA Nucleobases, J. Chem. Theory Comput. 8 (8) (2012) 2682–2687, https://doi.org/10.1021/ct300420f.

[44] A. Prlj, B.F.E. Curchod, A. Fabrizio, L. Floryan, C. Corminboeuf, Qualitatively Incorrect Features in the TDDFT Spectrum of Thiophene-Based Compounds, J. Phys. Chem. Lett. 6 (1) (2015) 13–21, https://doi.org/10.1021/jz5022087.

[45] E. Tanis, E.B. Sas, M. Kurban, M. Kurt, The structural, electronic and spectroscopic properties of 4FPBAPE molecule: Experimental and theoretical study, J. Mol. Struct. 1154 (2018) 301–318, https://doi.org/10.1016/j.molstruc.2017.10.057.

[46] B. Gunduz, M. Kurban, Photonic, spectroscopic properties and electronic structure of PTCDI-C8 organic nanostructure, Vib. Spectrosc. 96 (2018) 46–51.

[47] M.-T. Praet, J. Delwiche, Ionization energies of some cyclic molecules, Chem. Phys. Lett. 5 (9) (1970) 546–548, https://doi.org/10.1016/0009-2614(70)85041-2.

[48] K. Kimura, K. Kimura, Handbook of HeI Photoelectron Spectra of Fundamental Organic Molecules: Ionization Energies, Ab Initio Assignments, and Valence Electronic Structure for 200 Molecules, Halsted Press, Japan Scientific Societies Press, New York, Tokyo, 1981.

[49] K. Watanabe, T. Nakayama, J. Mottl, Ionization potentials of some molecules, J. Quant. Spectroscopy Radiat. Transfer 2 (4) (1962) 369–382, https://doi.org/10.1016/0022-4073(62)90023-7.